

# Extending the Application of One-Terminal Fault Location Method Available in Actual Time Domain Relay

Gustavo A. Cunha,\* Felipe V. Lopes,\* Tiago R. Honorato\*

\* *Department of Electrical Engineering, University of Brasilia, DF,  
(e-mail: gustavocunha@lapse.unb.br)*

---

**Abstract:** Traveling wave-based fault location has attracted more and more attention from industries worldwide. This theory allowed the implementation of functions in order to increase the reliability of the obtained fault location results. Among existing functions, the classical one-terminal method requires the detection of the wave reflected from the fault, which is still considered a challenging task. A commercial relay was released with a function able to identify these reflected waves by evaluating patterns and weighted hypotheses, identifying the wavefront most likely to be the one reflected from the fault. However, as this function is embedded into a relay, it is not possible to change the method settings. Thus, this paper presents a validation of this function which is implemented externally to the relay. Besides, its application is extended for transmission lines to which the relay can not be applied, such as huge HVDC lines.

*Keywords:* Electromagnetic Transients, Traveling Waves, Fault Location, Transmission Lines, Transient Detection Sensitivity.

---

## 1. INTRODUCTION

In order to speed up the system restoration after transmission line (TL) faults, many researches have focused on the topic of fast and accurate fault location. Several solutions have been reported with the aim of finding out efficient methods, and among them, methods based on traveling waves (TW) have been widely discussed, showing to be promising (Saha et al., 2010).

Most TW-based methods reported in the literature are classified as one- or two-terminal techniques, which have different advantages and limitations. Although the two-terminal method, in general, requires data synchronization and a couple of devices, its results tend to be more accurate and reliable, since they require the detection of only the first wavefront at both line ends. On the other hand, the one-terminal method requires only one equipment and it is independent of time synchronization. However, there are many challenges for this method, such as the requirement to identify waves reflected from the fault point (Gale et al., 1993).

A one-terminal method that demands neither TW velocity nor time synchronization is reported by Schweitzer et al. (2018). In order to properly operate, this method detects the first incident TW, together with the second and third successive reflections from the fault location and remote terminal. However, if the reflection from the remote terminal is attenuated or if it does not exist, the performance of this method may be jeopardized and the results will not be reliable.

Guangbin et al. (2013) present an one-terminal method for double circuit lines. It detects waves returning to the monitored terminal by other possible paths, such as parallel lines. However, the problem of adjacent lines is still present. Another method, known as the classical one-terminal fault location method, requires the arrival time of the first TW and its reflection from the fault point. It depends also on the propagation speed of waves on the TL, which is usually obtained from line electrical parameters (Saha et al., 2010).

The main issue of the classical one-terminal fault location method is the detection of the TW reflected from the fault. For this reason, Guzmán et al. (2017) proposed a way to identify the fault-induced transient patterns, obtaining weighted hypotheses, even in the presence of adjacent transmission lines. This method is already used in commercial relays, which have shown to be promising.

The principle applied to identify the reflected wave is demonstrated in Guzmán et al. (2017) and then, the classical one-terminal fault location method is applied. According to SEL (2017), the relay is designed to operate on alternating current (AC) TLs with a line length (LL) limitation, since the TW line propagation time setting is limited to 1700  $\mu$ s. To overcome these limitations, it is possible to implement this method externally to the device, allowing the access to internal variables, and thus its extension to systems in which the relay application would not be feasible. The idea of this paper is to validate the implementation made of this function in a numerical program. Then, the method is adapted to locate high-impedance faults which are not expected to be located by the real relay function as well as to locate faults on lines longer than the relay settings allowed.

---

\* The authors would like to thank the Coordination for the Improvement of Higher Education Personnel (CAPES) for the financial support.

## 2. TW-BASED FAULT LOCATION

A TW is an induced electromagnetic transient which propagates toward both sides of the TL after faults. To better understand such phenomenon and its applicability, TWs propagation must be studied. By knowing the TW propagation speed and the line propagation time (TWLPT), which depend on TL parameters, it is possible to calculate the fault location with the classical one-terminal method if the wave reflected from the fault is found. Fig. 1 depicts the Bewley diagram (BEWLEY, 1931) of a system with adjacent lines, where a fault occurred within the second half of the TL, being  $M$  the fault distance from the local terminal, and  $Z_{AL}$  the adjacent line impedance.

Assume that the first local terminal incident TW is detected at the instant  $t_1$ , while the wave reflected from the fault is detected at  $t_6$ . It can be seen that between these instants, other waves reach the local terminal, among which there are reflections from the adjacent lines ( $t_2$  and  $t_4$ ) and from the remote end ( $t_3$  and  $t_5$ ). As a result, the algorithm must be able to distinguish waves reflected from the fault.

The one-terminal classical fault location method is calculated according to Guzmán et al. (2017) as:

$$M = \frac{t_6 - t_1}{2 \cdot TWLPT} \cdot LL. \quad (1)$$

According to (1), the final fault location is simple to calculate provided that all the required equation inputs are known. However, the main challenge is to reliably find the  $t_6$  time stamp due to the amount of TW coming from adjacent lines and remote bus. As a result, only if the reflected wave arrival time is calculated correctly and high sampling rate is used, the fault distance will be accurately calculated.

## 3. STUDIED ONE-TERMINAL TW-BASED FAULT LOCATION ALGORITHM

The main idea of the proposed single ended TW fault location (SETWFL) method reported in Guzmán et al. (2017) is to find out the wave reflected from the fault point,

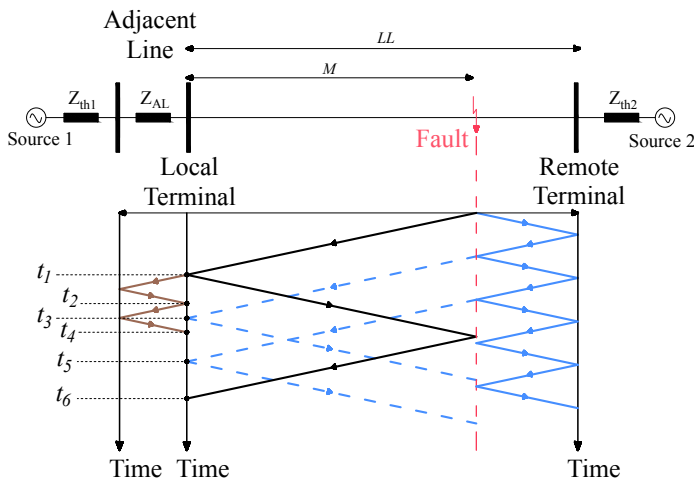


Figure 1. Bewley diagram.

i.e., identify the time stamp  $t_6$ , as in the example depicted in Fig. 1. Then the classical fault location method can be applied.

The studied SETWFL function is based on pattern recognition by weighting hypothesis for desired TW selection. However, before the methodology itself is applied, signal pre-processing is required to extract TW information from the measured signal. Besides sampling, the signal is decoupled by means of a modal transformation. For a three-phase system, Clarke's modal transformation is used here, as suggested in Guzmán et al. (2017). Then, the obtained  $\alpha$  ( $\alpha$ ),  $\beta$  ( $\beta$ ) and  $z$  ( $z$ ) modes are filtered via the Differentiator-Smoother filter, which is responsible for extracting TW information by converting fault-induced step changes into triangular shaped outputs (Ando et al., 1985; Lopes et al., 2019).

The original  $\alpha$  current after a single-phase fault and the DS filter outputs are depicted in Fig. 2. The fault induced TWs propagate throughout the transmission line, being reflected and refracted at system discontinuities, generating multiple TWs which are detected until their amplitudes diminish. As a consequence, the methodology sets an observation window on time called *Obs Window 1*, whose length is taken as  $2.4 \cdot TWLPT$  to select the peaks to be analyzed within a period enough to encompass the TW reflected from the fault.

Based on the *Obs Window 1*, the SETWFL algorithm is applied considering two methodologies: The Repeating Travel Time - RTT and Expected TW - ETW methodologies. These methods depend on hypothesis created by the algorithm, which analyzes the first incident TW polarity and compare it with the others TWs within the same of the first one, and it is identified within another defined observation window ( $Obs\ Window\ 2 = 2 \cdot TWLPT + TWTOL1$ ), then this wave is taken as a hypothesis, where  $TWTOL1$  is a tolerance normally equal to  $10\ \mu s$  (Guzmán et al., 2017). Although the *Obs Window 2* is within the *Obs Window 1*, the non shared peaks will not be used as a hypotheses, but will contribute for the patterns recognition calculation.

In Fig. 2, both observation windows are illustrated. Also, it is demonstrated that the second TW (second peak) will

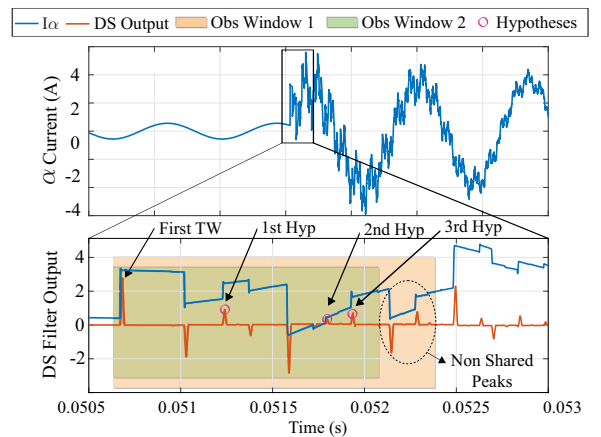


Figure 2. DS filter output and observation windows.

not be a hypothesis, since its polarity is opposite to the one of the first TW, even though it is within both observation windows. On the other hand, the third TW will be taken as a hypothesis, since it is within the *Obs Window 2* and its polarity is the same of the first TW. For this example, there are 3 hypotheses to be analyzed.

### 3.1 RTT Method

The goal of the RTT method is to prevent interference of TWs from adjacent lines on the wave of interest. TWs can refract to adjacent lines and reflect back to the monitored TL, resulting in more TWs measured at the monitored line terminal. Consequently, in order to provide a more reliable detection, this method calculates weights for each hypothesis. To calculate them, it is necessary to define an array, called DT, in which values are derived by the time difference between all the analyzed peaks, i.e., between peaks within the *Obs Window 1*. (Guzmán et al., 2017).

Once hypotheses are defined, the algorithm evaluates the amount of times the difference between the arrival time of the hypothesis and the first incident wave match the expected DT values, creating the weight  $NM(hyp)$ .

For each hypothesis, it is possible to calculate the refracted TW (time stamp  $t_3$  in Fig. 1) which is refracted from the fault point after being reflected from the remote terminal (such TW is called as a “companion” TW (Guzmán et al., 2017)). As a result, the number of times the difference between the companion TW and the first TW time stamps match with the DT values is analyzed, resulting in the  $N1\_M(hyp)$  weight (Guzmán et al., 2017).

### 3.2 ETW Method

The ETW method defines a weighting factor for each hypothesis, called  $WGHT(hyp)$ . It is a flag which is set to high logic value only if the companion TW exists. If this flag is activated, the algorithm creates the last weight, called  $NS(hyp)$  based on the number of times the measured TWs match with the expected TWs patterns for each hypothesis. These expected TWs are calculated by Bewley Lattice diagrams for each hypothesis. There are four main patterns that can be evaluated (Schweitzer et al., 2014), which are only taken into account if they are within the *Obs Window 1*.

### 3.3 SETWFL Final Fault Distance Estimation

The final weight is given by  $N(hyp)$ . To calculate  $N(hyp)$ , the SETWFL function divides the line into three sections. The first section is defined by 0 to  $0.3 \cdot LL$ . The second section is from  $0.3 \cdot LL$  to  $0.7 \cdot LL$ , and the third one is from  $0.7 \cdot LL$  to  $LL$  (Guzmán et al., 2017). Thus, if initial estimations from another fault location function is available, the faulted line section is used to calculate the final weight. Therefore, if the initial estimation is within the first line section,  $N(hyp)$  is calculated as (2) (Guzmán et al., 2017).

$$N(hyp) = NM(hyp). \quad (2)$$

If the initial estimation is within the second section, or if there is no fault location estimation from other function

available, the fault location function is applied as (3) (Guzmán et al., 2017):

$$N(hyp) = NM(hyp) + N1\_M(hyp) + WGHT(hyp) \cdot NS(hyp). \quad (3)$$

Lastly, if a fault is detected within the third section, the fault location function applies (4) (Guzmán et al., 2017):

$$N(hyp) = N1\_M(hyp). \quad (4)$$

The hypothesis with higher weight  $N(hyp)$  represents the function result, whose associated fault distance is taken as the SETWFL method output. Further details can be found in Guzmán et al. (2017).

## 4. SETWFL FUNCTION VALIDATION

The studied SETWFL is embedded in a commercial relay and its settings cannot be modified. Thus, to extend its application, as proposed here, it was implemented in a numerical calculation software, following the guidelines reported in Guzmán et al. (2017). By doing so, the fault location function was adapted for other types of TL and its sensitivity could be also improved.

### 4.1 Analyzed System

The function validation was carried out considering different types of faults on a TL with adjacent lines in order to present more realistic characteristics. Indeed, it creates the difficulty of determining which hypothesis corresponds to the reflected wave from the fault. The system was evaluated by means of the Alternative Transients Program (ATP) using the Bergeron line model with 230 kV/60 Hz and LL equal to 200 km. Fig. 3 depicts the analyzed power system, where the main and adjacent TLs parameters are shown. The Current Transformer used in this analysis is the CT C800 2000-5 proposed by IEEE-PSRC (2009) and that the Thévenin and adjacent line impedance were assumed to have the same parameters of the analyzed line.

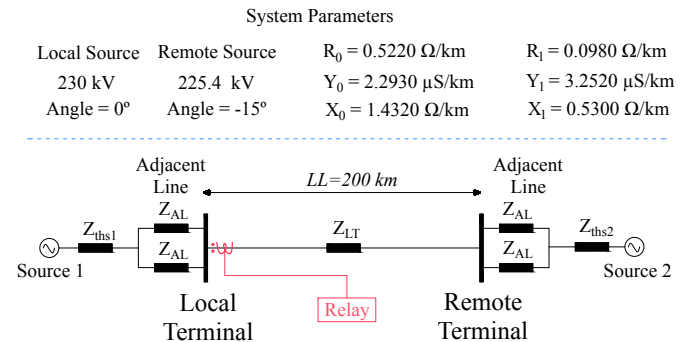


Figure 3. Analyzed System.

### 4.2 Validation

The SETWFL method performances were evaluated under different short-circuit scenarios, being  $R_f$  the fault resistance to ground:

- Single-phase fault ( $1\phi$ ) with  $R_f = 1 \Omega$ ;
- Single-phase fault ( $1\phi$ ) with  $R_f = 10 \Omega$ ;
- Double-phase fault to ground ( $2\phi g$ ) with  $R_f = 1 \Omega$ ;
- Double-phase fault to ground ( $2\phi g$ ) with  $R_f = 10 \Omega$ ;
- Solid Three-phase fault ( $3\phi$ ).

For each fault type, fault distances from 10% to 90% of the TL length with steps of 10% were simulated. In order to compare with the real relay results, standard COMTRADE files (IEEE-Std-C37.111, 2013) were also generated for all simulated events. The relay evaluation was carried out using the Event Playback functionality, which executes a COMTRADE file uploaded into the relay internal memory (Guzmán et al., 2018). This feature is crucial for TW testing due to the requirements of TW transient reproduction which are usually not met by standard testing equipment (Guzmán et al., 2018). In summary, the records of each simulated fault are sent to the relay, which processes the information, generating operation results that can be externally analyzed.

Regarding the methodology, due to the impossibility of isolating the SETWFL method in the relay, the same initial estimation was also provided for the implemented version in order to provide a fair comparison. The obtained results are presented in Figs. 4 and 5 where “Correct Result” is the exact point of the simulated fault, “SETWFL” represents the implemented algorithm results, and “Relay” stands for the relay results.

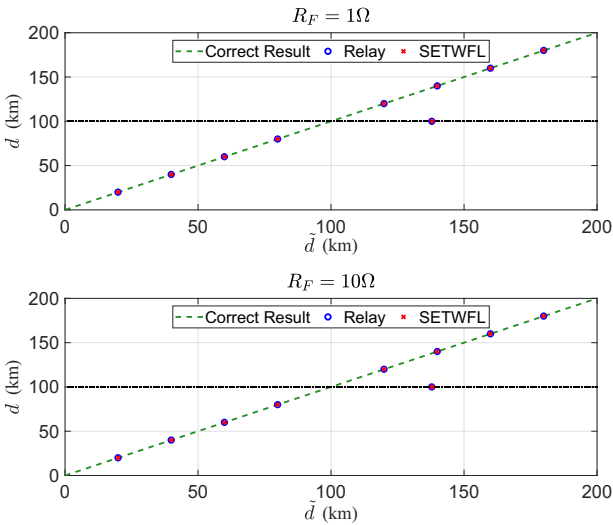


Figure 4. Single-phase fault.

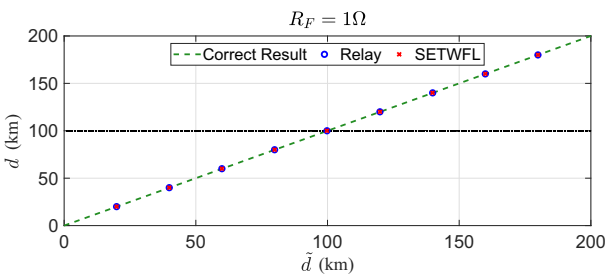


Figure 5. Three-phase solid fault.

The results demonstrate that the implemented SETWFL is in accordance with those obtained from the relay. Moreover, in Fig. 4, one may notice that a fault at the middle of the line yielded the same error in both relay and SETWFL implementation. Indeed, refracted waves at the fault point results in an opposite polarity compared to the reflected ones, overlapping each other and making its identification harder.

Additionally, to better understand the obtained results, the absolute errors between the implemented function and the relay function are analyzed. As depicted in Fig. 7, it can be seen that errors are negligible, being the maximum error of all simulated fault types smaller than 0.15 km. Just to have a comparison, the difference between the relay results and the implemented function was, in general, in the second decimal place, attesting the implemented SETWFL method is correct. Thus, the implemented SETWFL function was assumed to be validated allowing to evaluate, modify and even set the method for different applications to which the relay was not originally designed for.

## 5. EXTENDING APPLICATIONS OF THE SETWFL FUNCTION

Once the transient pattern recognition algorithm is validated, it is possible to cover a wider range of scenarios and systems, providing modifications to comply, for instance, with transmission lines with lengths greater than the maximum value supported by the relay, allowing its application

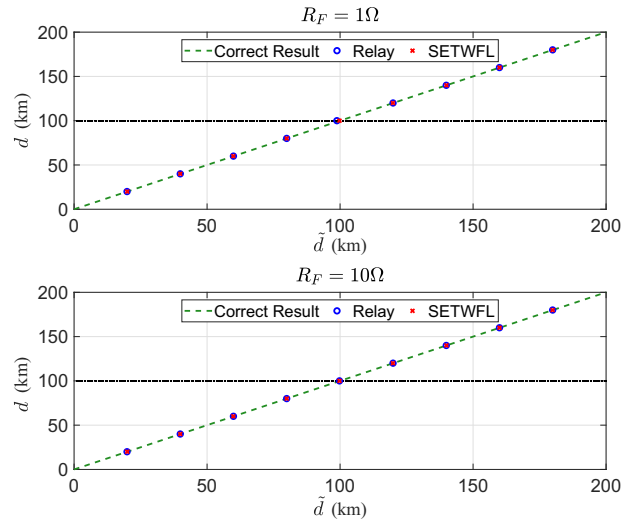


Figure 6. Double-phase fault.

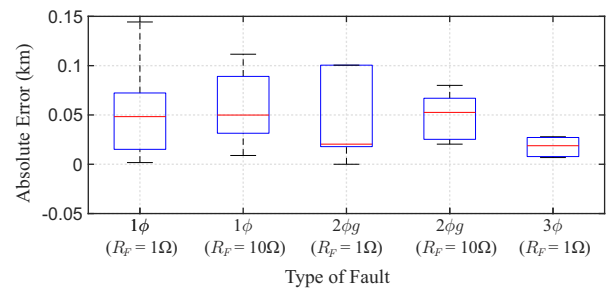


Figure 7. Absolute fault location error.

to huge High Voltage Direct Current (HVDC) TLs, for instance. Additionally, it is possible to customize the implementation in order to provide the adequate sensitivity that generate the most accurate fault location estimates for each system as analyzed in Cunha et al. (2019). As a result, to use the validated function in other types of TL, it is necessary to make internal changes such as threshold, weights and patterns, which would not be possible in the real relay.

The relay LL limitation is linked to the maximum line propagation time, which ranges from  $10.00 \mu\text{s}$  up to  $1700.00 \mu\text{s}$  (SEL, 2017). Assuming a TW at the speed of light equivalent to  $3 \cdot 10^5 \text{ km/s}$ , and considering the maximum value of the acceptable TW line propagation time, the maximum LL that the relay accepts, according to (5), is around 510 km.

$$LL = v \cdot \tau = 3 \cdot 10^5 \text{ km/s} \cdot 1700 \mu\text{s} = 510 \text{ km} \quad (5)$$

### 5.1 Applying to HVDC System

In order to test the one-terminal fault location function in HVDC lines, the benchmark HVDC system depicted in Fig. 8 was simulated in ATP software. This scheme stands for the Madeira River HVDC link, which has two bipoles with 3150 MW and 600 kV each. The interconnection stations are Coletora Porto Velho (Brazil) and Araraquara II (Brazil) (Luz et al., 2014.). This system model uses distributed and frequency independent line parameters with LL equal to 2450 km. Note that the HVDC system has a very long length, much longer than the maximum setting allowed by the relay. Even so, it is possible, with changes, to locate faults with the externally implemented SETWFL function.

Aiming to obtain promising results in this system, the threshold used to detect the TW after filtering signals via DS Filter was modified. In addition, Kahenbauer's modal transformation was used, instead of Clarke's one, since it is a direct current (DC) system with only positive and negative poles. As it is an HVDC system, TL terminations trap transients within the terminals, so that there is no concern about waves reflected from adjacent lines,

facilitating the location of the waves reflected and refracted from the fault (Zhang et al., 2011). For this reason, the function weights were changed in order to highlight more the refracted wave, since there is no concern about waves from adjacent TL, giving more weight to those hypotheses. Summarizing, for each hypothesis, it is analyzed if the companion wave exists, multiplying the *WGHT* value by 10, modifying the final weight *N*. Table 1 shows the differences between the relay and the implemented function for HVDC lines.

With this function reformulation, fault distances from 5% to 95% with steps of 5% in all the TL were simulated, considering a fault resistance to ground equal to  $1 \Omega$ . The results are shown in Fig. 9. Note that all blue markers were near the expected results, showing that the implementation of the SETWFL function with those modifications worked well. On the other hand, note that for a fault at the middle of the TL, no hypothesis has been identified with this method, since there is a superposition of reflected and refracted waves with opposite polarities, making it not possible to identify the TWs of interest. Still analyzing Fig. 9, it can be seen that the absolute error did not exceed 0.8 km, showing that the obtained results were accurate.

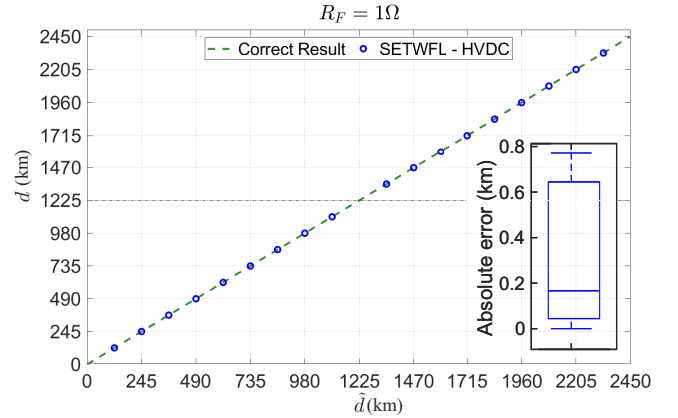


Figure 9. HVDC results.

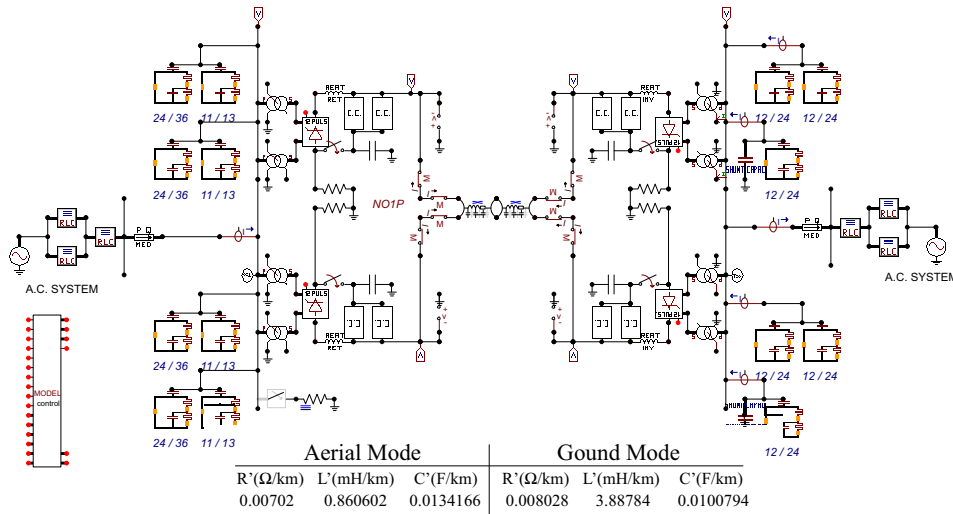


Figure 8. Madeira River HVDC link.

Table 1. Relay versus HVDC parameters

	Relay Parameters	HVDC Parameters
Modal Transformation	Clarke	Kahenbauer
Refraction TW Weight	$1 \cdot WGHT$	$10 \cdot WGHT$
Line Length Limit	Yes - 510 km	No limitation

## 5.2 Analyzed Threshold

In order to analyze the TW detection sensitivity at the fault location function, the same AC circuit depicted in Fig. 3 was simulated, considering a fault at 30% (60 km) of LL, with high resistance to ground equal to 160  $\Omega$  was considered. In this case, the real relay one-terminal TW fault location did not operate. Therefore, the same case was simulated to locate the fault using the implemented function, but reducing the TW detection threshold.

Due to the high resistance of the fault compared with the same type of fault without resistance, all the TW are attenuated, which makes it difficult, depending on the sensitivity, to properly detect the TW of interest. Since the function discussed here depends on weighting when the refracted TW is detected, modification of this threshold has shown to be a viable solution (Cunha et al., 2019).

The obtained result for this simulation was a fault location estimation at 61.4945 km with a threshold of 10 A, while the first TW had an amplitude equal to 190.1 A. It is noticeable that the threshold was quite small compared to the first TW amplitude. However, the hypothesis with greater weight was the correct one, demonstrating that the obtained approach also works for cases with high fault resistances using a simple algorithm modification. It is important to point out that the location error was 1.4945 km, which is equivalent to a relative error of 2.49%. Although it is an error larger than those usually obtained by means of TW functions, the result is coherent, with accuracy acceptable if the high TW attenuation is taken into account.

## 6. CONCLUSION

In this work it was shown the validation of the implemented SETWFL function. It was demonstrated that the implementation worked as expected, presenting results similar to the commercial device, even when the fault location scheme fails.

Once the function was validated, it was applied to a different type of circuit to which the real relay was not designed for, such as HVDC TL, with lengths greater than 510 km. In addition, the fault location for high fault resistances, which led the real relay to fail, has been successfully performed. For this case, the function threshold was varied, which is not an accessible variable in the real relay.

In this way, it was possible to validate the implemented function with the results obtained via actual relay, allowing to access internal variables not settable in the real device. In addition, it was possible to extend the methodology application for HVDC TL, also making it more sensitive in cases in which the real device may fail.

## REFERENCES

- (2017). *SEL T400L Ultra high speed transmission line relay traveling wave fault locator high resolution event recorder*. Schweitzer Engineering Laboratories.
- Ando, M., E. O. Schweitzer, I., and Baker, R.A. (1985). Development and field-data evaluation of single-end fault locator for two-terminal hvdc transmission lines - part 2 : Algorithm and evaluation.
- BEWLEY, L.V. (1931). Traveling waves on transmission systems.
- Cunha, G.A., Lopes, F.V., and da Rocha Honorato, T. (2019). Influence of traveling wave detection sensitivity on transient pattern recognition-based single-ended fault location approach. In *2019 Workshop on Communication Networks and Power Systems (WCNPS)*, 1–5. doi:10.1109/WCNPS.2019.8896342.
- Gale, P.F., Crossleya, P., Bingyin, X., G. Yaozhong, B.C., and Barker, J. (1993). Fault location based on travelling waves. *Proc. 5th Int. Conf. Develop. Power Syst. Protection*, 54–59.
- Guangbin, Z., Hongchun, S., and Jilai, Y. (2013). Traveling wave fault location for transmission lines based on arrival time difference of dominant fault induced current waves in closed loop circuit.
- Guzmán, A., Smelich, G., Sheffield, Z., and Taylor, D. (2018). Testing traveling-wave line protection and fault locators.
- Guzmán, A., Kasztenny, B., Tong, Y., Mynam, M.V., and Schweitzer Engineering Laboratories, I. (2017). Accurate and economical traveling-wave fault locating without communications.
- IEEE-PSRC (2009). *Understanding Microprocessor-Based Technology Applied to Relaying*. IEEE POWER SYSTEM RELAYING COMMITTEE.
- IEEE-Std-C37.111 (2013). Ieee/iec measuring relays and protection equipment part 24: Common format for transient data exchange (comtrade) for power systems - redline. *IEEE Std C37.111-2013 (IEC 60255-24 Edition 2.0 2013-04) - Redline*, 1–136.
- Lopes, F., Jr., E.L., Ribeiro, J.P., Lopes, L., Piardi, A., Otto, R., and Neves, W. (2019). Using the differentiator-smoother filter to analyze traveling waves on transmission lines: Fundamentals, settings and implementation.
- Luz, G.S., Junior, D.S.C., and Junior, S.G. (2014.). Hvdc transmission line modeling analysis in pscad and atp programs.
- Saha, M.M., Izykowski, J., and Rosolowski, E. (2010). Fault location on power networks.
- Schweitzer, E.O., III, A.G., Mynam, M., Skendzic, V., Kasztenny, B., Gallacher†, C., and Marx, S. (2018). Accurate single-end fault location and line-length estimation using traveling waves.
- Schweitzer, E.O., Guzmán, A., Mynam, M.V., Skendzic, V., and Bogdan Kasztenny, Schweitzer Engineering Laboratories, I. (2014). Locating faults by the traveling waves they launch.
- Zhang, Y., Tai, N., and Xu, B. (2011). A travelling wave protection scheme for bipolar hvdc line. In *2011 International Conference on Advanced Power System Automation and Protection*, volume 3, 1728–1731. doi:10.1109/APAP.2011.6180649.